

Comparative First-Principles Spin-Polarized DFT Study of Structural, Electronic, and Bonding Properties of $KRTe_2$ ($R = Al, In$) Using WIEN2k and CASTEP: Insights into Band Gap Nature, Ionic-Covalent Bonding, and Spin-Orbit Coupling Effects

Zahid Ullah^{1,2}, Muhammad Amir Khan¹, Sabahat Gul^{1,2}, Mohammad Noman².

1. Faculty of Physical and Numerical Sciences, Qurtuba University of Science and Information Technology, Peshawar/D.I. Khan, Pakistan.

2. Physics Department, Islamia College University, Peshawar, Pakistan.

Email: zuzohaad@gmail.com (Zahid Ullah), makphy83@gmail.com (Muhammad Amir Khan).

December 7, 2025

Abstract

Comparative first-principles spin-polarized DFT analysis of the structural, electrical, and bonding characteristics of $KInTe_2$ and $KAlTe_2$ is presented in this work. We investigate the direct and indirect band gap characteristics of these materials using the computer codes WIEN2k and CASTEP. Their potential for optoelectronic applications is shown by the alignment of their valence band maximum (VBM) and conduction band minimum (CBM) at the Γ point. An ionic-covalent interaction is revealed by the bonding study, with aluminium/indium-tellurium compounds showing strong covalent properties and potassium-tellurium bonds mostly being ionic. Additionally, the study takes into account spin-orbit coupling (SOC) effects, especially in $KInTe_2$, where heavier elements like tellurium and indium cause considerable SOC, which results in greater electronic anisotropy and dramatic band splitting. The findings imply the materials' suitability for spintronic and photovoltaic applications and emphasize the significance of SOC in altering the materials' electrical behaviour. Their technical value is further increased by the doping that allows their electrical properties to be tuned.

Keywords: Bonding nature, Structural, Bandgap, DFT, WIEN2k, CASTEP.

1. Introduction

The development of next-generation technologies, especially in the domains of flexible electronics, thermoelectrics, and optoelectronics, has made the investigation of new semiconductor materials essential. High-performance devices like solar cells, infrared sensors, magnetic sensors, and flexible electronic circuits require materials with exceptional structural, optical, and electrical properties, such as $KAlTe_2$ and $KInTe_2$. These chalcogenide compounds provide a unique blend of structural stability, non-toxic content, and customizable band gaps, which fits in nicely with the global trend toward efficient and ecologically friendly energy sources [1-2]. The increasing interest in low-dimensional materials for contemporary electronics makes research into compounds like $KAlTe_2$ and $KInTe_2$ even more pertinent, since they hold great promise for upcoming advancements in smart technology and renewable energy.

Two-dimensional (2D) semiconductors' remarkable flexibility, quantum confinement effects, and improved transport capabilities have brought about a revolution in material research in recent years. A-B-X-type compounds,

including KAlTe_2 and KInTe_2 , have garnered the most attention among them. According to their structural makeup, these materials crystallize in a layered tetragonal phase in which aluminum (Al) or indium (In) establish covalent connections with tellurium (Te) and potassium (K) interacts ionically with Te. According to theory, their distinct electrical structures are related to this mixed bonding feature [3-7]. Even though their fundamental structural and electrical configurations have been examined in earlier research, it is imperative to comprehend their thermodynamic behavior, magnetic interactions, and optoelectronic responses in a range of physical scenarios. Given their potential for effective heat-to-electricity conversion, these materials should also show encouraging thermoelectric qualities.

In crucial areas, KAlTe_2 and KInTe_2 are still not well studied despite their encouraging properties. Their anisotropic character is one of their main drawbacks, which can make it difficult to integrate them into useful devices by causing variations in mechanical and electrical performance across several crystallographic directions. Additionally, there is a conspicuous lack of experimental confirmation for the majority of the insights that are currently accessible, particularly with regard to their temperature-dependent, magnetic, and thermoelectric properties, which are based on theoretical modeling. A thorough grasp of their full potential is lacking, according to the literature, especially when it comes to the impact of spin-orbit coupling (SOC), which is essential for figuring out the electronic structure and magnetic behavior of materials that contain heavy elements like Te and In [8-11]. Deeper computational and experimental studies are therefore required to test these predictions, exposing a substantial research gap in the existing scientific environment.

Therefore, the goal of this work is to close this knowledge gap by carefully examining how spin-orbit coupling affects the structural and electrical characteristics of KInTe_2 and KAlTe_2 . This work aims to shed light on SOC effects in order to shed light on their electrical band structures, magnetic interactions, and possible spintronic uses. Among the particular goals is the analysis of the SOC-induced modifications to magnetic behavior, density of states, and band dispersion with respect to thermoelectric and optoelectronic performance [12-14]. This research could help build new semiconductor devices that are suited to local needs, like flexible electronics and solar harvesting, in Pakistan's local context of creating environmentally friendly and energy-efficient technology. This paper's ultimate goal is to provide a fundamental knowledge of the spin-orbit coupling effects in these materials, opening the door for further advancements in materials engineering and semiconductor physics.

2. Methods of Calculation

It is possible to examine material qualities through both theoretical and experimental methods. Properties are frequently investigated experimentally through the analysis of wave functions obtained from the Schrödinger Wave Equation. The Kohn-Sham Equation serves as the theoretical foundation for Density Functional Theory (DFT), which offers a potent framework for material investigation. DFT-based methods are essential for investigating the electrical, structural, and spin-orbit coupling features of materials. One of the most popular DFT techniques for evaluating complicated materials like KAlTe_2 and KInTe_2 is the Full-Potential Linearized Augmented Plane Wave (FP-LAPW) approach, which is implemented in computer programs like WIEN2k and CASTEP. This approach works especially well for giving precise computations of a material's electrical structure and bonding properties. The Generalized Gradient Approximation (GGA), more especially the GGA-PBEsol functional, is frequently used to characterize the exchange-correlation energy in structural research [15-17]. Because of its reputation for producing accurate data regarding the structural characteristics of materials, the GGA-PBEsol functional is highly valued. The band gap is a crucial metric to consider while examining the electrical properties. Standard GGA functionals are frequently used to determine the band gap for conductors, semiconductors, insulators, and superconductors.

Although GGA offers accurate band gap estimates, it is known to underestimate band gaps in some materials, especially insulators and semiconductors. Because of this restriction, more sophisticated functionals have been created inside the GGA framework with the goal of more accurately representing electrical structures in various

material kinds. These developments aid in overcoming obstacles to more accurate modelling and material property prediction. Furthermore, to comprehend magnetic behaviour and relativistic effects in systems including heavy elements like tellurium and indium, first-principles spin-polarized DFT simulations that incorporate spin-orbit coupling effects are crucial. Spin-orbit coupling effects are also incorporated into other DFT techniques, including as the Local Density Approximation (LDA), meta-GGA, and hybrid functionals, each of which has special advantages in handling the electronic and relativistic behaviours of complex systems [18–21].

3. Results and Discussion

In this section we are investigating the structural, bandgap and Bonding properties of ternary telluride.

3.1. Structural Properties

Using the full-potential Linearized Augmented Plane Wave (FP-LAPW) approach in the context of density functional theory (DFT), the structural properties of tetragonal materials, in particular the ternary tellurides KAlTe_2 and KInTe_2 , were examined [22–23]. The Generalized Gradient Approximation (GGA) and this approach, which is renowned for its accuracy, were used to precisely calculate the equilibrium unit cell volumes and evaluate the materials' chemical makeup.

In the tetragonal space group $I4/mcm$ (No. 140), KAlTe_2 and KInTe_2 crystallize. Te atoms occupy the 8h Wyckoff positions with coordinates (0.1645, 0.6645, 0), K atoms are located at the 4a sites with coordinates (0, 0, 0.25), and Al or In atoms are located at the 4b sites with coordinates (0, 0.5, 0.25), according to their unit cell structures, which are displayed in Figures (1) and (2) using two computational codes. These configurations provide intricate and unique structural components that influence the crystal lattice's overall shape and bonding.

Four Te atoms centrally coordinate Al or In atoms in a somewhat deformed tetrahedral geometry to generate XTe_4 tetrahedral units within the structure. Furthermore, eight Te atoms create a quadratic antiprism around each K atom, enclosing the K atoms within KTe_8 octahedral units. The coordinating environment in these materials is highlighted by these arrangements, which are depicted in Figures (1) and (2).

According to crystallography, the type of lattice affects the coordination number (CN). Because of its denser atomic packing, a face-centered cubic (FCC) lattice has a CN of 12, whereas a body-centered cubic (BCC) lattice has a CN of 8. As a transitional phase, the body-centered tetragonal (BCT) structure is a warped version of the cubic lattice. Depending on the degree of distortion and the particular atomic arrangement, its coordination number might vary from 8 to 12.

The delicate interaction between symmetry, bonding, and atomic packing in the tetragonal system is shown by the structural intricacy of KAlTe_2 and KInTe_2 , which are distinguished by their tetrahedral and octahedral coordinating units. This work shows how well the FP-LAPW approach and GGA work together to capture the intricate structural and electrical aspects of these cutting-edge chalcogenide materials.

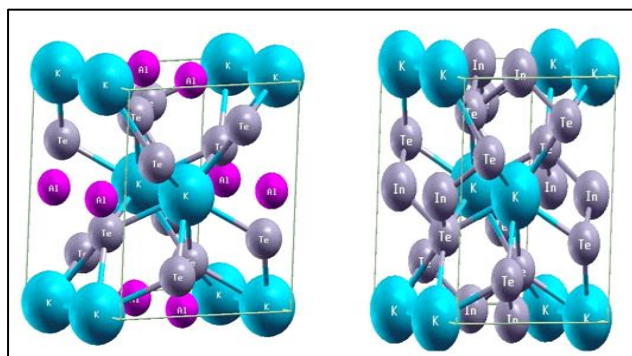


Figure 1. Unit cells of the investigated materials, $KAlTe_2$ and $KInTe_2$, as modeled using the WIEN2k code within the DFT framework.

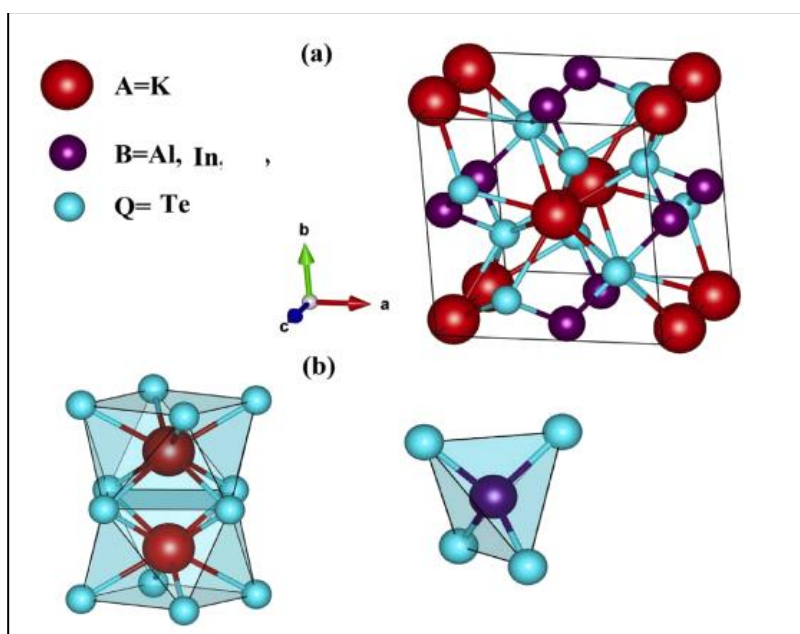


Figure 2. Unit cells of the investigated materials, $KAlTe_2$ and $KInTe_2$, as simulated using the CASTEP code based on density functional theory.

Table 1. Experimental and theoretical lattice parameters (a in Å and c in Å) for ternary compounds crystallized in the tetragonal space group $I4/mcm$ (No. 140), calculated using the GGA potential.

Compounds	Experimental	Present	Wyckoff	Positions
$KAlTe_2$	$a=b= 8.77$	8.69	K	(0 ,0, 0.25)
	$c=6.71$	7.00	Te	(0.1645,0.6645,0)

KInTe_2	$a=b= 8.76$	8.52	Al/In	(0, 0.50, 0.25)
	$c= 7.43$	7.39		

3.2. Optimisation Properties

Energy–volume (E – V) charts for KAlTe_2 and KInTe_2 are shown in Figure 3. These plots were computed using the density functional theory (DFT) framework and the WIEN2k algorithm. With each curve exposing a minimum point corresponding to the equilibrium volume (V_0), which represents the most stable configuration at 0 K and 0 pressure, these plots show total energy (in Rydberg) as a function of unit cell volume (in a.u.³) [24–25]. KInTe_2 exhibits a greater equilibrium volume than KAlTe_2 , which is consistent with the larger atomic size of In relative to Al. The predicted parabolic shape near the minima implies structural stability.

The figure caption is unclear in spite of these advantages. The graphs itself merely display energy vs volume; there is no clear indication of how the c/a ratio was handled, despite the mention to "varying percent c/a ratios." It should be made explicit if the atomic locations and c/a ratio were relaxed at each fixed volume (Interpretation A), as is customary. If not, the reader can mistakenly believe that the approach represents fixed c/a calculations or simultaneous volume and c/a variation in a 2D graphic, which is not possible.

The treatment of relativistic effects (particularly crucial for heavy elements like Te and In), the exchange–correlation functional (e.g., PBE, PBEsol), convergence criteria (e.g., k-point mesh, RKmax), and whether internal atomic coordinates were fully relaxed are among the other crucial computational details that are absent. Furthermore, fitting the data to an equation of state (EOS), like Birch–Murnaghan, which would enable the extraction of the bulk modulus (B_0) and other significant parameters, is not mentioned.

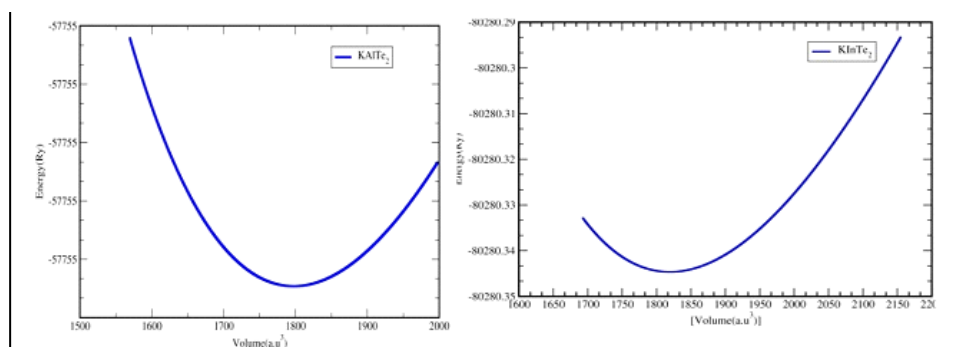


Figure 3. Energy optimization plots of KAlTe_2 and KInTe_2 using the WIEN2k code, illustrating energy changes with varying percent c/a ratios.

3.3. Band Structure

Although tellurides are intrinsic semiconductors by nature, they can be doped with elements like potassium (K), aluminum (Al), or indium (In) to become extrinsic semiconductors with adjustable electrical characteristics. The band gap, which controls a material's electrical and optical characteristics, is one of the most important factors in semiconductor physics. Density of states (DOS) plots provide an approximate approximation of the band gap, but they do not reveal whether the gap is direct or indirect [26–27]. Analyzing the band structure across different high-symmetry sites in the Brillouin zone is crucial to figuring out the nature of the band gap.

When the conduction band minimum (CBM) and valence band maximum (VBM) line up at the same symmetry point, usually the Γ point, a direct band gap results. On the other hand, when the VBM and CBM are situated at different symmetry points, there is an indirect band gap. The band structures of KAlTe_2 and KInTe_2 , respectively, are computed using the Generalized Gradient Approximation (GGA) in the DFT framework employing two computational codes, as shown in Figures (4) and (5). With the VBM and CBM aligned at the Γ point, these band structures unequivocally show that both materials have direct band gaps. For reference, the Fermi level is given as 0.0 eV.

The direct band gap nature of KAlTe_2 is confirmed by the CBM and VBM lying within the first Brillouin zone at the Γ point using the WIEN2k code. KInTe_2 exhibits direct band gap properties as well, with important contributions from important symmetry points including R, Γ , X, and M. In strong agreement with previous DFT-based investigations, the GGA-calculated band gaps are 1.67 eV for KAlTe_2 and 0.915 eV for KInTe_2 . As indicated in Table 2, additional refinement with the HSE06 hybrid functional produces more precise values of 2.126 eV and 1.845 eV, respectively.

When calculated using the CESTEP code, the CBM and VBM for KAlTe_2 are found at the Γ point within the first Brillouin zone, confirming its direct band gap nature. Likewise, KInTe_2 exhibits direct band gap properties, with important contributions from R, Γ , X, and M, among other important symmetry points. In good agreement with previous DFT-based investigations, the GGA-calculated band gaps for KAlTe_2 and KInTe_2 are 1.68 eV and 0.931 eV, respectively. As shown in Table 3, additional refining with the HSE06 hybrid functional yields more precise band gap estimates of 2.157 eV and 1.858 eV for KAlTe_2 and KInTe_2 , respectively.

These outcomes demonstrate the materials' potential for use in optoelectronic applications and support the efficacy of the computational method. They are perfect for photovoltaic cells, light-emitting diodes (LEDs), and other devices that need high transparency or accurate light absorption because of their straight band gap. Their use in next-generation electrical and optoelectronic technologies is improved by the doping that allows their electronic characteristics to be tuned.

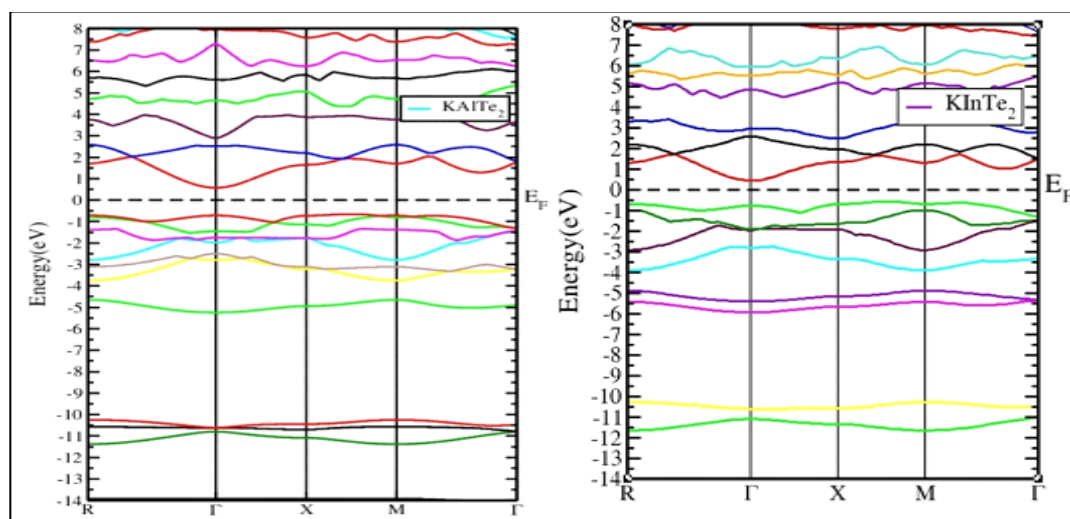


Figure 4. Band structures of the investigated materials computed using WIEN2k code, showing direct band gaps at the Γ point for KAlTe_2 and KInTe_2 .

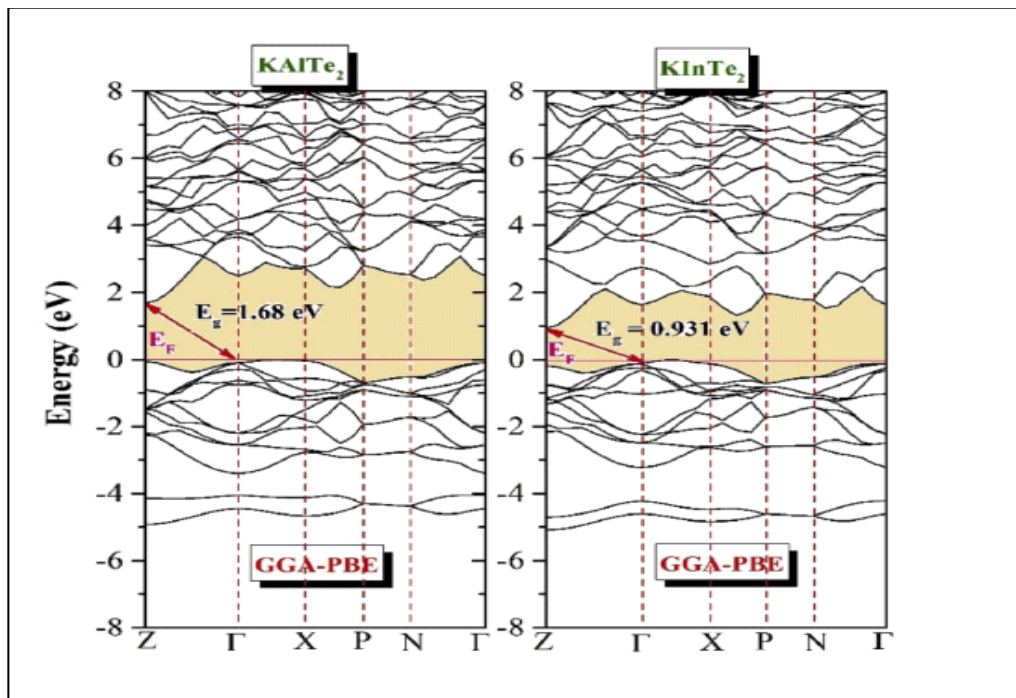


Figure 5. Band structures of the studied materials using CASTEP code, illustrating direct band gaps at the Γ point for $KAITE_2$ and $KInTe_2$.

Material	Method	GGA Calculated Band Gap (eV)	HSE06 Refined Band Gap (eV)
$KAITE_2$	WIEN2k	1.67	2.126
$KInTe_2$	WIEN2k	0.915	1.845
$KAITE_2$	CASTEP	1.68	2.157
$KInTe_2$	CASTEP	0.931	1.858

Table 2. Comparing the GGA-calculated and HSE06-refined band gaps (in eV) for $KAITE_2$ and $KInTe_2$ using WIEN2k and CASTEP codes. The values demonstrate the direct band gap nature of both materials, with the HSE06 hybrid functional yielding more accurate band gap estimations compared to the GGA calculations.

3.4. Bonding Nature/ Electron Charge Density

The electron density charts in Figure (6) offer crucial information on the charge transfer and bonding characteristics of the KAlTe_2 and KInTe_2 crystal structures. These plots provide a thorough perspective of how electrons are shared or localized inside the structure by displaying the electron density distribution throughout the materials. This data enables a more thorough examination of the materials' electrical properties and is essential for comprehending the kinds of links that exist between the different ions [28]. According to two computer algorithms, the electron density surrounding the potassium ion in KAlTe_2 is almost spherical, indicating that the potassium-tellurium connection is mostly ionic in character. As an alkali metal, potassium has a tendency to create ionic connections with electronegative metals such as tellurium, which is compatible with this discovery. Tellurium ions are more inclined to receive electrons and produce negatively charged ions, whereas potassium has a tendency to lose electrons and generate a positive ion, as indicated by the spherical electron cloud surrounding it. Consequently, the interaction between potassium and tellurium is primarily ionic.

The electron density pattern surrounding the tellurium and aluminum atoms in KAlTe_2 , on the other hand, exhibits a more directed bonding behavior, which is typical of covalent connections. Strong electron sharing and a highly localized electron cloud surrounding these atoms suggest a covalent relationship. Tellurium and aluminum form a covalent connection that is necessary for the material's electrical and structural stability. Similar to this, the indium-tellurium bond in KInTe_2 has a strong covalent nature, with the electron density between the indium and tellurium atoms being more localized. But like KAlTe_2 , the potassium-tellurium link in KInTe_2 is still primarily ionic. When A is an alkali metal and B and X are different elements, this pattern is consistent with the general bonding pattern seen in other A-B-X_2 systems. As indicated in Table 3, the A-X bonds (such as potassium-tellurium) are primarily ionic in these structures, but the B-X bonds (such as aluminum-tellurium or indium-tellurium) are typically covalent.

Both theoretical predictions and practical results for comparable materials are supported by these bonding properties. The stability and electrical characteristics of KAlTe_2 and KInTe_2 are greatly influenced by their distinct ionic-covalent bonding behavior. The materials' structural stability and electrical behavior are influenced by the interaction between ionic and covalent bonds, which is essential for their possible uses. These materials are especially well-suited for usage in cutting-edge technologies like photovoltaic devices, optoelectronic applications, and nonlinear optical devices due to their unique charge transfer characteristics and bonding nature. Because of their distinct structural and electrical features, KAlTe_2 and KInTe_2 are becoming more and more attractive options for future study and technological advancement in response to the growing need for materials with particular electronic properties.

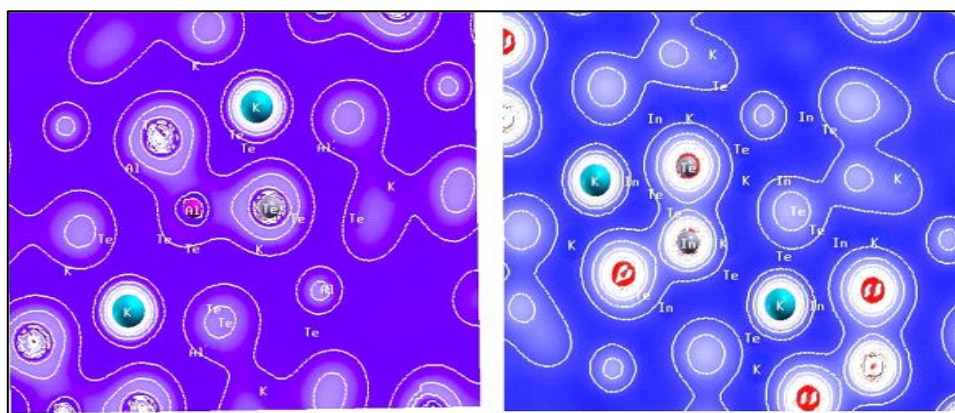


Figure 6 illustrates the bonding nature of KAlTe_2 and KInTe_2 , analyzed using WIEN2k and CESTEP codes, highlighting the ionic and covalent interactions within their crystal structures.

Material	Bonding Type (Potassium-X)	Bonding Type (Aluminum/Indium-X)
KAlTe_2	Ionic	Covalent
KInTe_2	Ionic	Covalent

Table (3) summarizing the ionic bonding between potassium and tellurium, and the covalent bonding between aluminum/indium and tellurium in KAlTe_2 and KInTe_2 , as analyzed using WIEN2k and CESTEP codes.

3.5. Spin Orbit Coupling (SOC)

A significant relativistic effect in materials containing heavy elements is spin-orbit coupling (SOC), which results from the interplay between an electron's orbital motion around the nucleus and its spin. SOC has a major impact on the electrical structure, especially the band gap and magnetic behavior, in compounds such as KAlTe_2 and KInTe_2 . A robust framework for precisely including SOC effects without the need for empirical input is provided by first-principles spin-polarized density functional theory (DFT) [29-30]. SOC in these materials may be precisely evaluated thanks to computational codes like CASTEP, which uses plane-wave pseudopotentials, and WIEN2k, which is based on the full-potential linearized augmented plane wave (FP-LAPW) approach. Relativistic pseudopotentials in CASTEP and a second-variational approach in WIEN2k are commonly used to incorporate SOC, which enables in-depth examination of spin patterns, density of states (DOS), and electronic band structures.

The SOC contributions in KAlTe_2 and KInTe_2 are associated with the electronic arrangements of the atoms. While heavier atoms like tellurium (Te: $[\text{Kr}] 4d^{10} 5s^2 5p^4$) and indium (In: $[\text{Kr}] 4d^{10} 5s^2 5p^1$) play a dominating role in SOC, light atoms like potassium (K: $[\text{Ar}] 4s^1$) and aluminum (Al: $[\text{Ne}] 3s^2 3p^1$) contribute very little. Because of their hefty atomic weights and partially filled 5p and 4d orbitals, Te and In both add considerable SOC effects, which cause noticeable band splitting close to the Fermi level, especially in KInTe_2 . Increased electronic anisotropy, altered band gap behavior, and possible spintronic applications are the outcomes of this. Therefore, it is crucial to accurately include SOC in order to comprehend and customize the practical characteristics of these intriguing materials.

4. Conclusion

In conclusion, two computational codes, WIEN2k and CESTEP, were used to analyze KAlTe_2 and KInTe_2 . This analysis yielded important information about the structural, electrical, and bonding properties of these materials. Both materials are perfect for optoelectronic applications because they have direct band gaps, as shown by their computed band structures, with the valence band maximum (VBM) and conduction band minimum (CBM) aligned at the Γ point. These materials' bonding properties show a mix of covalent and ionic interactions. Aluminum-tellurium and indium-tellurium bonds have significant covalent properties, but potassium-tellurium bonds in both KAlTe_2 and KInTe_2 are primarily ionic. The electrical stability and structural integrity of the materials are greatly enhanced by this ionic-covalent bonding activity. Moreover, the incorporation of spin-orbit coupling (SOC) improves our comprehension of the electrical characteristics, especially in KInTe_2 , where heavy elements like

tellurium and indium produce strong SOC effects that result in band splitting and possible spintronic uses. Both materials' electrical behavior is significantly influenced by their tetragonal crystal structure, which is defined by tetrahedral and octahedral coordination units. These results highlight how KAlTe₂ and KInTe₂, with doped electronic properties that can be adjusted, are suitable for advanced applications in photovoltaics, optoelectronics, and nonlinear optics. They are promising materials for upcoming technological advancements because of their special bonding and electrical properties.

5. Data availability Statement

All data generated or analyzed during this study are fully included in this article, ensuring transparency and reproducibility of the research findings. "Data will be made available on request"

6. Funding Declaration

"This research was conducted without any external funding support." This research received no specific grant from any funding agency in the public, commercial, or not-for-profit sectors.

7. Declaration of competing interest

The authors declare no competing financial interests or personal relationships that could influence the work reported in this paper. Zahid Ullah states that no financial support was received from any funding agency. Other authors have no known competing interests to disclose.

8. Acknowledgements

The authors, including Zahid Ullah and co-authors, gratefully acknowledge the support and facilities provided by the Faculty of Physical and Numerical Sciences, Qurtuba University of Science and Information Technology, Peshawar/D.I. Khan, Pakistan, and the Physics Department, Islamia College University, Peshawar, Pakistan. Their resources and encouragement greatly contributed to the successful completion of this research.

9. Copyright Notice

This article is published by the Author under a Creative Commons CC-BY 4.0 license. The Authors retains full copyright, with the first publication right granted to the London Journal of Physics.

References

1. Bouchenafa, M., Benmakhlouf, A., Sidoumou, M., Bouhemadou, A., Maabed, S., Halit, M., Al-Douri, Y. Theoretical investigation of the structural, elastic, electronic, and optical properties of the ternary tetragonal tellurides KBTe₂ (B = Al, In). *Mater. Sci. Semicond. Process.* 114, 105085–105088 (2020). <https://doi.org/10.1016/j.mssp.2020.105085>
2. Benmakhlouf, A., Bentabet, A., Bouhemadou, A., Maabed, S., Khenata, R., Bin-Omran, S. Structural, elastic, electronic, and optical properties of KAlQ₂ (Q = Se, Te): A DFT study. *Solid State Sci.* 81, (2015). <https://doi.org/10.1016/j.solidstatesciences.2015.02.003>
3. Ullah, Z., Amir, M., Bazilla, A., Ullah, S., Shahzad, U., Ullah, N., Gul, S. Electronic, thermoelectric and magnetic properties of ternary tellurides KAlTe₂ and KInTe₂ from a theoretical perspective. *Next Res.* 100077, (2024). <https://doi.org/10.1016/j.nexres.2024.100077>

4. Belgoumri, G., Bentabet, A., Khenata, R., Bouhadda, Y., Benmakhlouf, A., Rai, D.P., Bounab, S. Insight into the structural, electronic and elastic properties of AInQ₂ (A = K, Rb; Q = S, Se, Te) layered structures from first-principles calculations. *Chin. J. Phys.* 56(3), 1074–1088 (2018). <https://doi.org/10.1016/j.cjph.2018.04.009>
5. Benmakhlouf, A. Structural, elastic, electronic and optical properties of KAlQ₂ (Q = Se, Te): a DFT study. *Solid State Sci.* 48, 72–81 (2015). <https://doi.org/10.1016/j.solidstatesciences.2015.07.006>
6. Feng, K.K. Synthesis, structure, physical properties, and electronic structure of KGaSe₂. *Solid State Sci.* 14(8), 1152–1156 (2012).
7. Kim, J., Hughbanks, T. Synthesis and structures of ternary chalcogenides of aluminum and gallium with stacking faults: KMQ₂ (M = Al, Ga; Q = Se, Te). *J. Solid State Chem.* 149(2), 242–251 (2000). <https://doi.org/10.1006/jssc.1999.8523>
8. Witt, C.W., Shires, W.B., Tan, W.C., Jankowski, J.W., Pickard, J.C. Random structure searching with orbital-free density functional theory. *J. Phys. Chem. A* 125(7), 1650–1660 (2021). <https://doi.org/10.1021/acs.jpca.0c11030>
9. Trani, F., Ninno, D., Cantele, G., Iadonisi, G., Hameeuw, K., Degoli, E., Ossicini, S. Screening in semiconductor nanocrystals: Ab initio results and Thomas-Fermi theory. *Phys. Rev. B* 73(24), 245430 (2006). <https://doi.org/10.1103/PhysRevB.73.245430>
10. Xie, Q.X., Wu, J., Zhao, Y. Accurate correlation energy functional for uniform electron gas from an interpolation ansatz without fitting parameters. *Phys. Rev. B* 103, 045130 (2021). <https://doi.org/10.1103/PhysRevB.103.045130>
11. Claeys, C., Hsu, P.C., Mols, Y., Han, H., Bender, H., Seidel, F., Simoen, E. Electrical activity of extended defects in relaxed In_xGa_{1-x}As hetero-epitaxial layers. *ECS J. Solid State Sci. Technol.* 9, 033001 (2020). <https://doi.org/10.1149/2162-8777/ab74c7>
12. Ikeda, A., Koibuchi, S., Kitao, S., Oudah, M., Yonezawa, S., Seto, M., Maeno, Y. Negative ionic states of tin in the oxide superconductor Sr_{3-x}SnO revealed by Mössbauer spectroscopy. *Phys. Rev. B* 100, 245145 (2019). <https://doi.org/10.1103/PhysRevB.100.245145>
13. Tran, F. WIEN2k: an augmented plane wave plus local orbitals program for calculating crystal properties. (2018).
14. Madsen, G.K.H., Singh, D.J. BoltzTraP: a code for calculating band-structure dependent quantities. *Comput. Phys. Commun.* 175, 67–71 (2006). <https://doi.org/10.1016/j.cpc.2006.03.007>
15. Wu, C.S., Lee, P.Y., Chai, J.D. Electronic properties of cyclacenes from TAO-DFT. *Sci. Rep.* 6, 37249 (2016).
16. Engel, J., Francis, S., Roldan, A. The influence of support materials on the structural and electronic properties of gold nanoparticles—a DFT study. *Phys. Chem. Chem. Phys.* 21, 19011–19025 (2019).
17. Feng, S., Wang, N., Li, M., Xiao, H., Liu, Z., Zu, X., Qiao, L. The thermal and electrical transport properties of layered LaCuOSe under high pressure. *J. Alloys Compd.* 861, 157984 (2021). <https://doi.org/10.1016/j.jallcom.2020.157984>
18. Wiebeler, H. A linear scaling DFT-method and high-throughput calculations for p-type transparent semiconductors. Doctoral dissertation, Universitätsbibliothek (2020).
19. Schwarz, K., Blaha, P. Solid state calculations using WIEN2k. *Comput. Mater. Sci.* 28, 259–273 (2003). [https://doi.org/10.1016/S0927-0256\(03\)00112-5](https://doi.org/10.1016/S0927-0256(03)00112-5)
20. Schwarz, K. DFT calculations of solids with LAPW and WIEN2k. *J. Solid State Chem.* 176(2), 319–328 (2003). [https://doi.org/10.1016/S0022-4596\(03\)00213-5](https://doi.org/10.1016/S0022-4596(03)00213-5)
21. Labrim, H., Jabar, A., Laanab, L., Jaber, B., Bahmad, L., Selmani, Y., Benyoussef, S. Optoelectronic and thermoelectric properties of the perovskites: NaSnX₃ (X = Br, I)—a DFT study. *J. Inorg. Organomet. Polym. Mater.* 33(10), 3049–3059 (2023).

22. Selmani, Y., Labrim, H., Mouatassime, M., Bahmad, L. Structural, optoelectronic and thermoelectric properties of Cs-based fluoroperovskites CsMF₃ (M = Ge, Sn, Pb). *Mater. Sci. Semicond. Process.* 152, 107053 (2022). <https://doi.org/10.1016/j.mssp.2022.107053>
23. Bouhmaid, S., Marjaoui, A., Talbi, A., Zanouni, M., Nouneh, K., Setti, L. A DFT study of electronic, optical and thermoelectric properties of Ge-halide perovskites CsGeX₃ (X = F, Cl, Br). *Comput. Condens. Matter* 31, e00663 (2022). <https://doi.org/10.1016/j.cocom.2022.e00663>
24. Ribeiro, R.A., Andres, J., Longo, E., Lazaro, S.R. Magnetism and multiferroic properties at MnTiO₃ surfaces: a DFT study. *Appl. Surf. Sci.* 452, 463–472 (2018). <https://doi.org/10.1016/j.apsusc.2018.05.067>
25. Madsen, H., Singh, J.D. BoltzTraP: A code for calculating band-structure dependent quantities. *Comput. Phys. Commun.* 175(1), 67–71 (2006). <https://doi.org/10.1016/j.cpc.2006.03.007>
26. Kaur, T., Sinha, M.M. Probing thermoelectric properties of high potential Ca₃PbO: An ab initio study. *IOP Conf. Ser. Mater. Sci. Eng.* 1033(1), 012080 (2021). <https://doi.org/10.1088/1757-899X/1033/1/012080>
27. Mahmood, Q., Hassan, M., Ahmad, S.H., Bhamu, K.C., Mahmood, A., Ramay, S.M. Study of electronic, magnetic, and thermoelectric properties of AV₂O₄ (A = Zn, Cd, Hg) by using DFT approach. *J. Phys. Chem. Solids* 128, 283–290 (2019). <https://doi.org/10.1016/j.jpcs.2017.08.007>
28. Feng, S., Wang, N., Li, M., Xiao, H., Liu, Z., Zu, X., Qiao, L. The thermal and electrical transport properties of layered LaCuOSe under high pressure. *J. Alloys Compd.* 861, 157984 (2021). <https://doi.org/10.1016/j.jallcom.2020.157984>
29. Ribeiro, R.A., Andres, J., Longo, E., Lazaro, S.R. Magnetism and multiferroic properties at MnTiO₃ surfaces: A DFT study. *Appl. Surf. Sci.* 452, 463–472 (2018). <https://doi.org/10.1016/j.apsusc.2018.05.067>
30. Benmekideche, N., Bentabet, A., Bouhadda, Y., Boubatra, D., Belgoumri, G., Fetah, S., Benyelloul, K. DFT study of structural, electronic and elastic properties of two polymorphs of monoclinic CsGaQ₂ (Q = S, Se). *Chin. J. Phys.* 56(3), 1345–1352 (2019). <https://doi.org/10.1016/j.cjph.2018.03.006>